Determination of mean sea surface and sea level anomaly models in different regional and temporal scales by altimetric data[1]

G.S. Vergos and D.A Natsiopoulos

Department of Geodesy and Surveying, Aristotle University of Thessaloniki, University Box 440, 541 24, Thessaloniki, Greece, Fax: +30 31 0995948, E-mail: vergos@topo.auth.gr

Abstract: The exploitation of altimetric data sets from past and current satellite missions is crucial to both oceanographic and geodetic applications, since it allows the determination of sea level anomalies, as deviations from a static mean sea level, while it is also fundamental for geoid determination. In this paper, altimetric data sets from the satellite missions of Jason1 and ENVISAT have been used towards the determination of Mean Sea Surface (MSS) models in the Mediterranean Sea. The main aim though is to use the raw Sea Level Anomaly (SLA) values and their total inverse barometer corrections from the respective altimetric missions to study SLA change. In this respect, along-track records of the SLA have been used to derive linear trends of the SLA variation in the area under study in short time intervals between 10 and 35 days. Empirical covariance functions and the statistical analysis of the SLA along-track repeated satellite records are presented and are finally used to estimate a mean sea surface model, which is then compared with the DTU2010 model.

Keywords: satellite altimetry, mean sea surface, sea level anomalies, covariance functions.

1. Introduction

From the early missions of GEOS-3 and SeaSat in the mid '70s to the recent ones of Jason-2 and ENVISAT, altimeters onboard satellites offer an unprecedented database of instantaneous measurements of the sea surface. The basic altimetric measurement refers to the satellite height above the non-static sea surface, determined as the two-way travel time needed for the radar pulse emitted from the satellite to reach the sea surface and received by the instrument's receiver (see Figure 1, AVISO 2011). The difference between that height and the altitude of the satellite above a reference ellipsoid leads to the determination of the instantaneous sea surface height (SSH), which successfully represents the geometric height of the non-

[1] *Part of this work was prepared by the second author in the frame of his Diploma Thesis (Natsiopoulos 2010)*

static sea surface. This abundance of measurements for the Earth's oceans lead to an improved knowledge of the monitoring of sea level variations over large time and spatial scales. Repeated satellite altimetry data span nowadays over a period of about 35 years, if one considers the exact repeat mission (ERM) of GEOSAT as a landmark and the latest missions of JASON-2 and ENVISAT. This record of measurements about the variations and mean level of the Earth's oceans, manage to provide reliable monitoring tools for time periods as short as ten days, useful for sea level anomaly determination, and long enough in order to provide a more-or-less reliable estimate of trends in mean sea level (MSL) rise (Chelton et al. 2001).

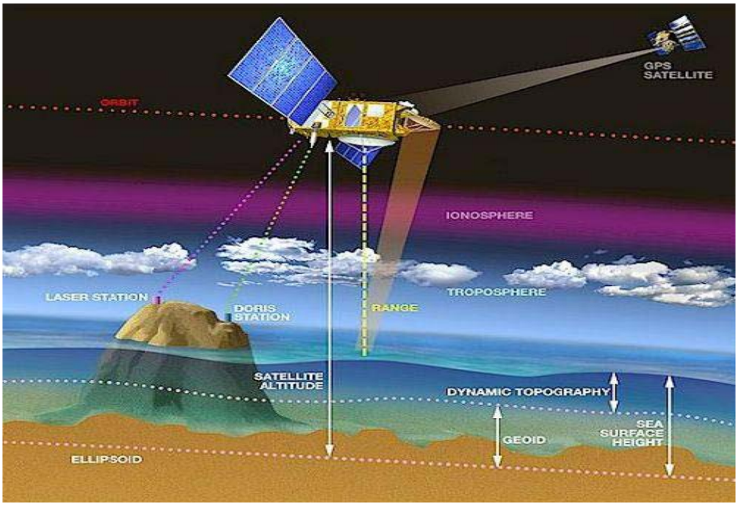

Figure 1. **Principle of satellite altimetry**

As far as the determination of mean sea surface (MSS) models from satellite altimetry data is concerned, many studies have been conducted in the past, presenting either global models (Andersen and Knudsen 1998, 2008; Cazenave et al. 1996; Yi 1995) or regional ones (Arabelos and Tziavos 1996; Tziavos et al. 1998; Vergos 2002; Vergos et al. 2005a,b,2007), the latter mainly in the form of altimetric marine geoid models. Satellite altimetry observations have provided for the first time homogeneous and almost-global coverage, high-resolution and precision observations for the instantaneous sea surface compared to the traditional shipboard data. Therefore, they offer a powerful tool in order to monitor and model processes that take place on the surface of the oceans (sea level variations, rise/fall, ocean circulation, etc.) (Cazenave and Nerem, 2004; Church et al., 2011; Nerem et al. 2006) and in their interior through inverse modeling (currents, temperature/salinity/pressure variations, etc.). A very good review on the applications of satellite altimetry to geodesy and sea level changes is given by Nerem and Mitchum (2001) and Tapley and Kim (2001) respectively.

Within the aforementioned frame, the aim of the present study is to first analyze available JASON1 and ENVISAT observations of sea level anomalies (SLAs) in the wider area of the Mediterranean Sea. Even though the Mediterranean is a semi-closed sea basin, with limited span especially in the north-south direction, the availability of repeated altimetric tracks allows monitoring of variations with time of the sea level at spans as short as the repeat period of the available satellite data. In that way, seasonal and temporal variations of the sea level can be studied, while conclusions on the existence of long-term trends can be derived as well. Given that the available data in the present study came from the JASON1 and ENVISAT missions, the variation of SLA within the repeat period of the former (10 to 20 day periods) has been investigated for selected cycle. The second goal is to develop MSS models based on single- and multi-mission satellite altimetry data using least squares collocation (LSC). The latter is well-established, especially in geodetic research as the leading estimation principle within a least squares prediction scheme, and is based on the determination of some output stochastic signal(s) based on the availability of input data which are inter-related with the outputs with some covariance function in the sense that all variance-covariance matrices for the adjustment are derived from one basic covariance function (Barzaghi et al. 2009a,b; Sansò et al. 2008). In LSC, and in order to construct the necessary covariance and cross-covariance matrices it is necessary to fit some analytical model to empirical values, so that within the scheme of the present study, the Tscherning and Rapp model was fitted to the empirical SLA covariance functions derived from the available data (Tscherning and Rapp 1974). Given that the selection of the correlation length is vital for the construction of the necessary covariance and cross-covariance matrices, a study of the varying behavior of the empirical covariance models was performed in relation to the cross- and along-track spacing of the available satellite data.

2. Area under study, available data and pre-processing

The area under study spans the entire Mediterranean Sea bounded between $30^{o} \leq \varphi \leq 50^{o}$ and $-10^{o} \leq \lambda \leq 40^{o}$. As already mentioned in the previous section, the data employed in the present work are those of the JASON1 and ENVISAT missions. For JASON1, data during the period from 15/1/2002 (cycle 1) to 07/12/2008 (cycle 255) have been used resulting in a total number of 670703 observations (see Figure 2 for the JASON1 data distribution). Each JASON1 cycle consists of 254 passes with almost 20% of those having available observations in the Mediterranean Sea within the satellite's period of 10 days. As far as ENVISAT is concerned, 678258 point values (see Figure 3 for the ENVISAT data distribution) have been collected, within the period 24/09/2002 and 25/03/2009 (cycle 1 to cycle 77). The mesh of values is much denser than JASON1 and is composed by about 1003 passes. Its cross track spacing is 75 km at the equator compared to 300 km for JASON1. The data used have been downloaded from the Radar Altimeter Database System (RADS) operated by the Delft Institute for Earth-Oriented Space research (DEOS) (RADS 2011). RADS presents a collection of almost all past and current satellite altimetry and is DEOS' effort in establishing a harmonized, validated and cross-calibrated sea level data base from satellite altimeter data. The selection of RADS to collect the JASON1 and ENVISAT observations was based on the facts that a) harmonized geophysical corrections for all data were needed compared to using various geophysical models, e.g. from AVISO for JASON1 (Aviso 1998), b) the SLAs datum in terms of the reference ellipsoid needed to be unified in order to avoid datum inconsistencies that would result in biases when computing multi-satellite solutions (Fernandes et al. 2006, Tziavos et al. 2005), c) the SLAs from both satellites were needed in a unified and commonly crossover adjusted orbit reference frame (see below on the selection of the orbit reference frame of the data used) and d) easiness and one-stop place data collection for both satellites.

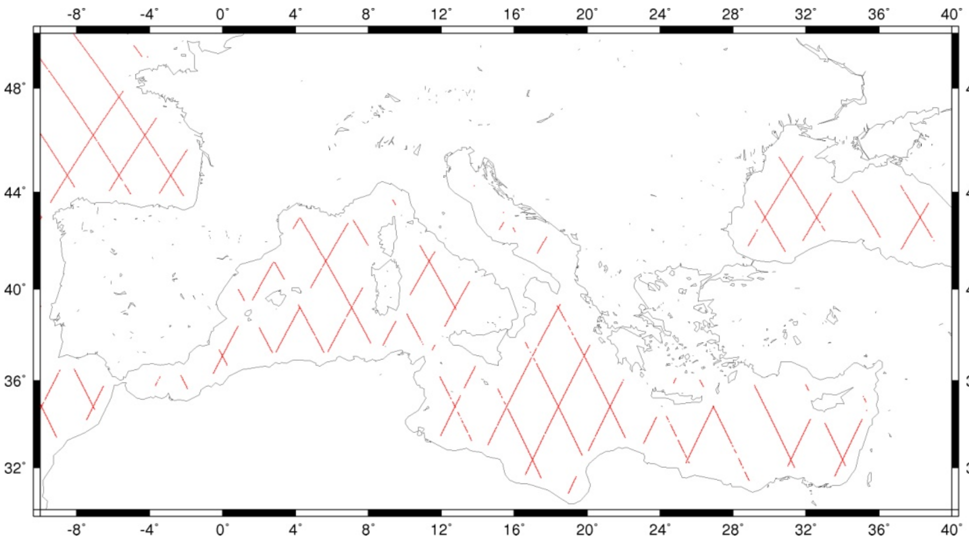

Figure 2. **JASON1 data distribution.**

The altimetric data were available in the form of SLAs referenced to a *"mean-sea-surface"* that depends on user selection within the RADS system. *Therefore,* it was decided to refer the data to the EGM2008 geoid (Pavlis et al. 2008)*, keeping in mind that a zero-tide (ZT) geoid model is adopted to be in-line with the tide-conventions used in altimetric data processing*. As far as the selection of the geo-physical corrections and models used, those were a) ECMWF for the dry tropo-spheric correction, b) MWR(NN) for the wet tropospheric correction, c) the smoothed dual-frequency model for the ionospheric correction, d) tidal effects due to Solid Earth, Ocean, Load and Pole from the Solid Earth tide, GOT4.7 ocean tide, GOT4.7 load tide and pole tide models respectively, and e) the CLS Sea State Bias (SSB) model for the SSB effect. Naeije et al. (2008) and the references herein should be advised for more details on the models used. All geophysical corrections mentioned previously have been applied to the JASON1 and ENVISAT raw observations, in order to construct corrected geophysical data records, i.e., corrected SLAs referenced to the EGM2208 ZT geoid.

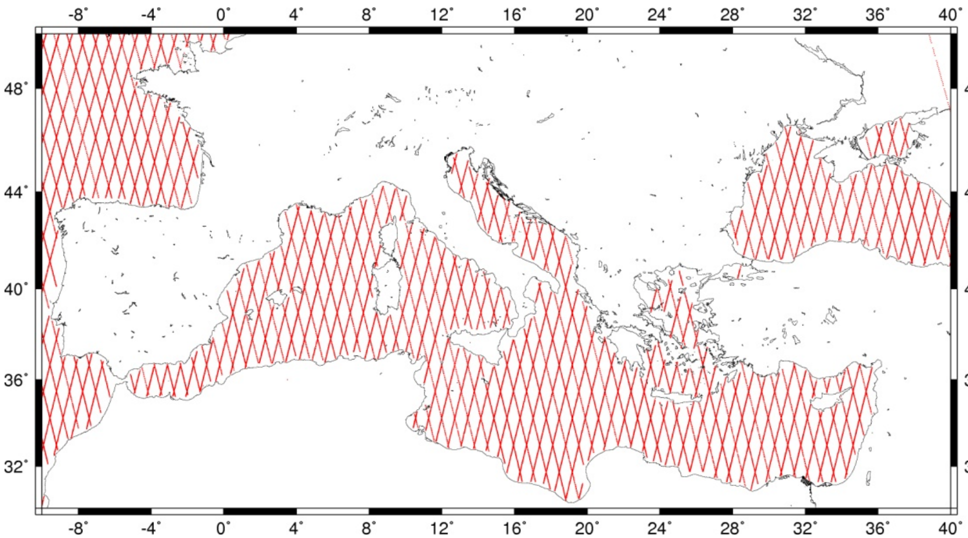

Figure 3**. Envisat data distribution.**

As far as the Inverse Barometer (IB) correction is concerned, this has been applied at a second stage to the available SLA data, during which, both the global and local IB corrections were applied. Tables 1 and 2 below summarize the statistics of the corrected SLA values for the geophysical effects, before and after the total inverse barometer corrections. From these Tables, it is obvious that the total inverse barometer correction has little effect to the "global" SLA statistics, i.e., the range of the values and their mean and standard deviation (std). The maximum and minimum values shown are clearly due to blunders in the available SLA data and they are located in all cases close to the coastline. Before proceeding any further to the utilization of the SLA data for MSL or sea level variations studies, a 3σ test has been applied in order to remove blunders. It should be noted that in order to apply such a blunder detection and

Table 1. Statistics of JASON1 data before and after the total IB correction. Unit: [m].

	nr. values	min	max	mean	std
SLA	653789	-1.817	0.880	0.009	±0.150
SLA+total inv. barom. cor	653789	-1.914	1.083	-0.044	±0.189

Table 2. Statistics of ENVISAT data before and after the total IB correction. Unit: [m].

	nr. values	min	max	mean	std
SLA	678255	-2.781	1.179	0.028	±0.143
SLA+total inv. barom. cor	678255	-2.748	1.315	0.078	±0.163

removal test, the data are regarded as bias free, which for the case of the JASON1 and ENVISAT observations holds since the mean value of the former is at the 9 mm level and that of the latter close to 3 cm. Such small mean values can be safely regarded as close to zero, so that the data can be treated as bias free. The meaning of the 3σ test is that all SLA values that exhibit a value of 3σ in an absolute sense, are regarded as blunders and are removed from the database. Table 3 below summarizes the statistics of the JASON1 and ENVISAT SLAs after the 3σ removal test (see the top row of Tables 1 and 2 for comparison). As far as JASON1 data are concerned, only 6344 (less than 1%) observations were removed as blunders, while the reduction of the data range is significant from ~2.6 m to 0.88 m only. From the ENVISAT SLAs, a total number of 8502 observations are removed (~1.2), again reducing the range of the data significantly, from ~3.9 m to 0.86 m only.

Table 3. Statistics of JASON1 and ENVISAT SLAs after the 3σ. Unit: [m].

	nr. values	min	max	mean	std
JASON SLAs	647445	-0.447	0.447	0.010	±0.141
ENVISAT SLAs	669753	-0.433	0.433	0.022	±0.133

These latter blunder-free observations will form the basis for the investigation of SLA variations and the determination of MSS models in the area under study.

3. Sea level anomaly variations in the Mediterranean Sea

The first part of this work refers to the identification of sea level variations within the satellite repeat period, i.e., for periods as short as 10 days (actually 9.9 days) for JASON and 35 days for ENVISAT. In order to investigate such variations, a single pass was selected from each satellite based on the following criteria: a) the pass shall be long and span the entire basin in the north-south or south-north direction (ascending or descending pass respectively), b) there shall be no or little land intrusion from isles or islands in the pass SLA records, c) the data record shall be as consistent as possible throughout the satellite data record for the period of study, i.e., missing records and/or voids should be kept to a minimum. Based on these criteria, it was decided that pass 196 would be studied for JASON1 and pass 399 for ENVISAT. JASON1 pass 196 is an ascending pass leaving Africa in the coastal areas of Libya, continuing north to the Ionian Sea and ending to the south-east part of Italy. On the other hand, ENVISAT pass 399 is a descending one crossing the entire eastern Aegean Sea, starting in the north off the coast of Thasos, crossing Lemnos, then east Cyclades, and finally after crossing the strait between Crete and Karpathos enters the Libyan Sea and ends over the coasts of Egypt. Figure 4 below depict the two passes investigated, where the red color denotes JASON1's pass 196 and the blue color ENVISAT's pass 399. The analysis presented herein refers to the aforementioned tracks for each satellite, therefore along-track SLA variations are studied rather than basin-wide.

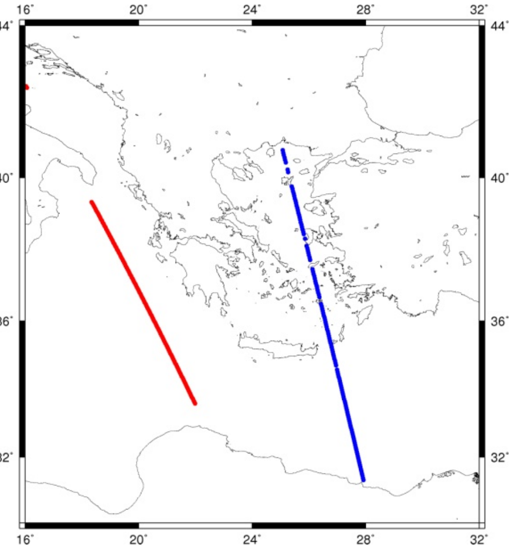

Figure 4. **JASON1 pass 196 (red) and Envisat pass 399 (blue) used for SLA variation monitoring.**

i. Sea level anomaly variations from JASON1

The study period for the JASON1 SLA data is between cycle 1 (15/01/2002) and cycle 255 (07/12/2008). Table 4 below summarizes the statistics of the annual JASON1 SLAs after the application of all geophysical corrections including that of the global and local IB ones. From that Table it is evident that the available annual JASON1 SLAs do not present a significant variation, since from 2002 until 2008 the std varies by ~2 cm, while some noticing variations can be viewed in the range of the observations only. Therefore it becomes apparent that a more detailed outlook per-cycle and track is needed in order to detect SLA variations.

Starting from cycle 1 for pass 196, the Figures and Tables given below present a) the available SLAs for the same pass and three consecutive cycles, so that a full month is covered (e.g., cycle 1 is analyzed together with cycles 2 and 3 so that a total of ~30 days is studied), and b) the SLA residuals between the studied cycles,

Table 4. Statistics of annual JASON1 SLAs.

YEAR	cycles	min	max	mean	std
2002	1-36	-0.472	0.771	0.018	±0.142
2003	37-73	-1.239	0.695	-0.007	±0.148
2004	74-110	-0.690	0.793	0.009	±0.164
2005	111-146	-0.631	0.690	0.011	±0.156
2006	147-183	-0.543	0.800	0.012	±0.152
2007	184-220	-1.817	0.880	-0.005	±0.136
2008	221-255	-0.842	0.791	0.021	±0.144

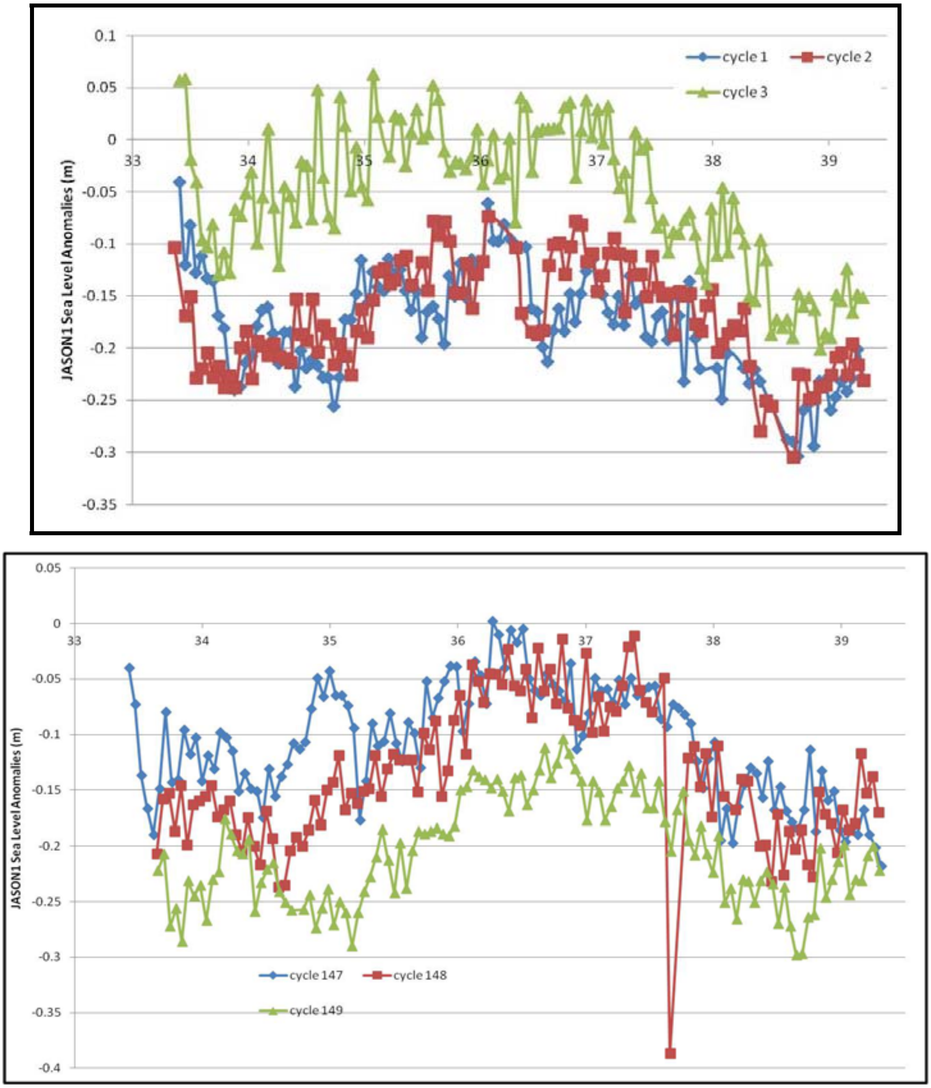

Figure 5. **JASON1 pass 196 SLAs for cycles 1, 2 and 3 (top), cycles 147, 148 and 149 (bottom).**

i.e., the differences between the available SLAs for the three consecutive cycles studied. Figures 5 and 6 present the available SLAs for pass 196 and cycles 1, 2 and 3 as well as their differences. In all Figures the horizontal axis refers to geographic latitude and the vertical one to SLAs or SLA differences in m.

From Figure 5 (top), it becomes evident that a good correlation between the SLA data between cycles 1 and 2 exists, while cycle 3 deviates significantly from the other two. This deviation can be viewed as a constant bias between the three cycles

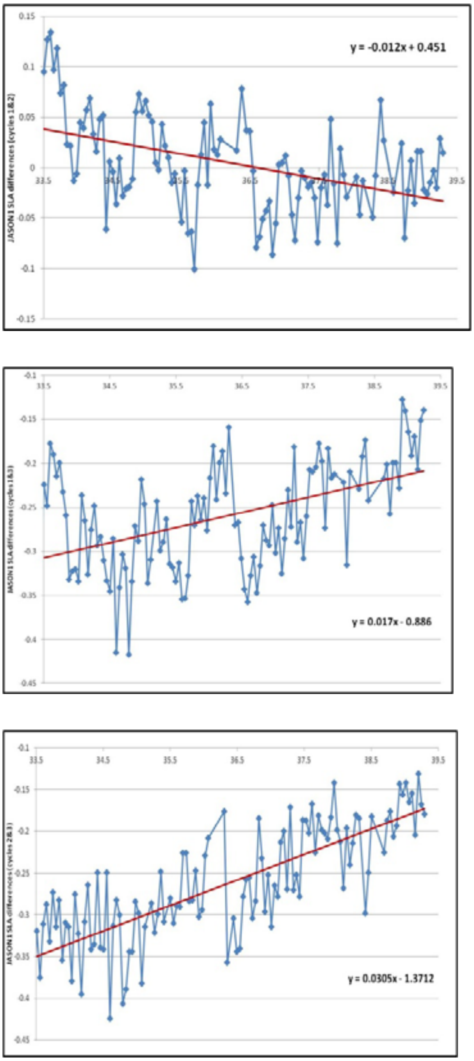

Figure 6. **JASON1 SLA differences and linear trend for pass 196 between cycles 1 and 2 (top), 1 and 3 (middle), 2 and 3 (bottom).**

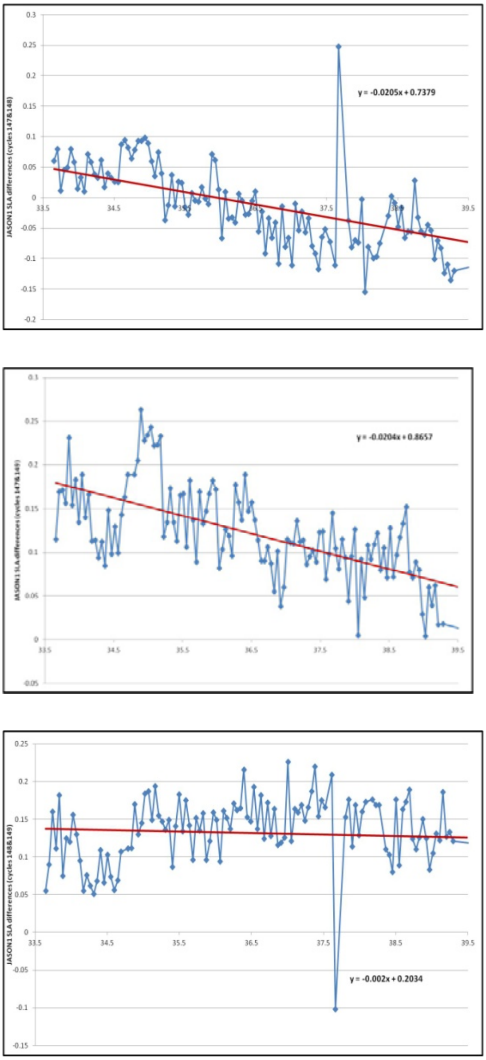

Figure 7. **JASON1 SLA differences and linear trend for pass 196 between cycles 147 and 148 (top), 147 and 149 (middle), 148 and 149 (bottom).**

of the order of 10 cm. It should be noted that the SLA data are already corrected for the IB effect, so this deviation cannot be attributed to the sea surface response to the change of the air pressure. From Figure 6, where the SLA differences between cycles 1, 2 and 3 are plotted a linear trend, i.e., change in the sea level, between -1.2 cm and 3.1 cm per 9.9 days can be seen. The latter trend of 3.1 cm/10 days is found between cycles 2 and 3, signaling that a significant variation in the sea level occurred between these days. It should be noted that these cycles refer to January 2002, so the same analysis has been performed for available SLAs in January 2006 (cycles 147, 148 and 149) and January 2008 (cycles 221, 222 and 223).

From Figure 5 (bottom), the same good correlation between cycles 147 and 148 (corresponding to cycles 1 and 2) can be found, while again cycle 149 (corresponding to cycle 3) presents a bias of the order of 15 cm. From Figure 7, a linear trend of -2.1 cm/30 days and -2 cm/10 days is found between cycles 147 and 149 and 147 and 148 respectively. This situation reverses in 2008 when analyzing cycles 221, 222 and 223 (corresponding to cycles 1, 2 and 3 respectively), since now the ones that are 30 days apart present a better correlation than the 10 day ones. The bias between the SLA data is now at the 10 cm level, while the trend ranges between 2.7 cm/10 days and 1.1 cm/20 days.

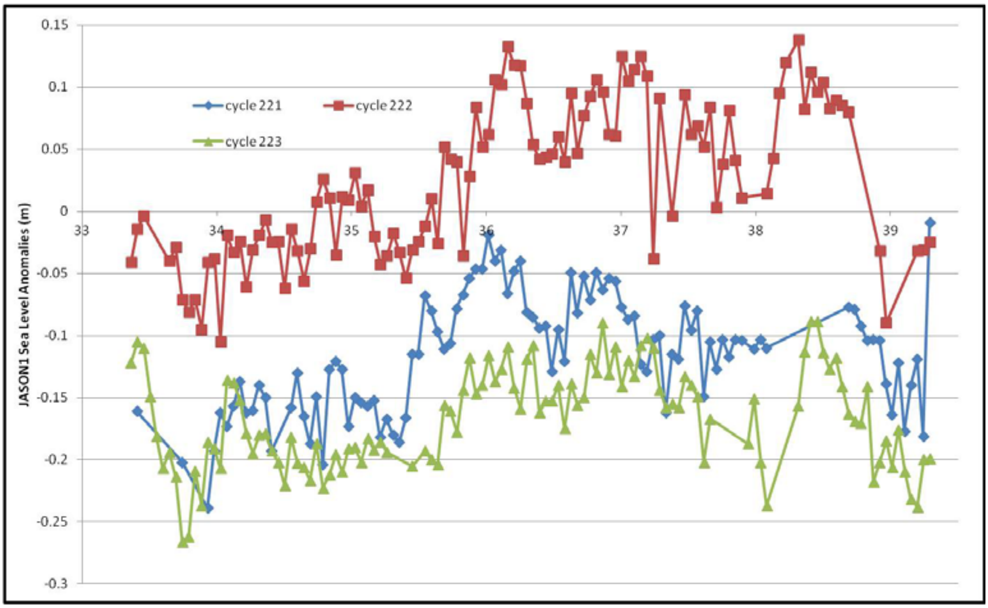

Figure 8. **JASON1 pass 196 SLAs for cycles 221, 222 and 223.**

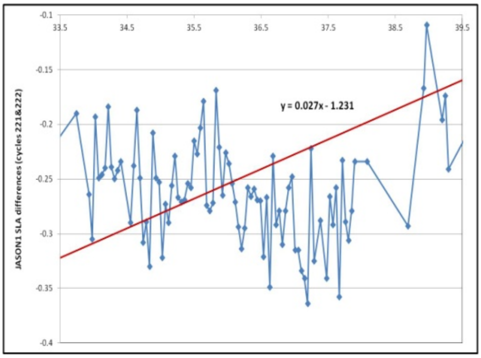

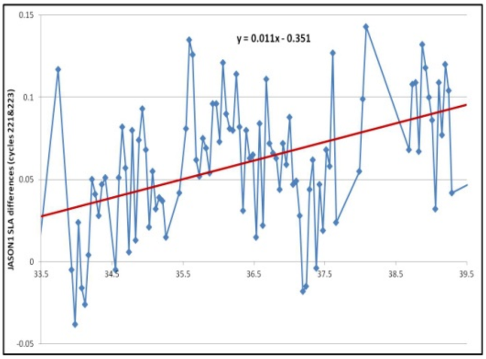

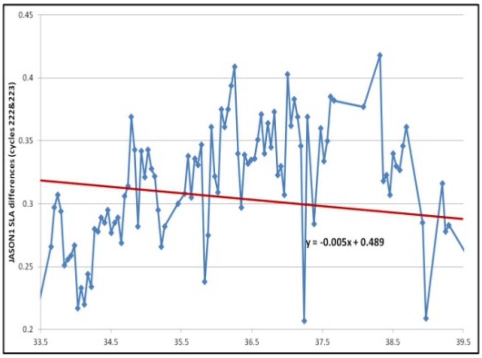

Figure 9. **JASON1 SLA differences and linear trend for pass 196 between cycles 221 and 222 (top right), 221 and 223 (top left), 222 and 223 (bottom).**

ii. Sea level anomaly variations from ENVISAT

The study period for the ENVISAT SLA data is between cycle 13 (13/03/2003) and cycle 75 (24/01/2009). Table 5 below summarizes the statistics of the annual ENVISAT SLAs after the application of all geophysical corrections including that of the global and local IB ones. From that Table a variation of the order of ~2 cm can be seen in the std, which is in agreement with the findings from JASON1. The large discrepancies in the minimum value of year 2007 can be attributed to same blunders still existing in the SLA records.

Table 5. Statistics of annual JASON1 SLAs.

YEAR	period	cycles	min	max	mean	std
2003	13-1-03 to 2-2-04	13-23	-0.773	0.911	0.013	±0.138
2004	2-2-04 to 17-1-05	24-33	-0.802	1.061	0.026	±0.154
2005	17-1-05 to 2-1-06	34-43	-1.142	1.179	0.029	±0.153
2006	2-1-06 to 22-1-07	44-54	-1.391	0.893	0.026	±0.149
2007	22-1-07 to 7-1-08	55-64	-2.781	0.792	0.028	±0.130
2008	7-1-08 to 24-1-09	65-75	-0.727	0.798	0.030	±0.134

Starting from cycle 23 for pass 399, the Figures and Tables given below present a) the available SLAs for the same pass and three consecutive cycles, so that more than three months are covered (e.g., cycle 23 is analyzed together with cycles 24 and 25 so that a total of ~105 days is studied), and b) the SLA residuals between the studied cycles, i.e., the differences between the available SLAs for the three consecutive cycles studied. It should be pointed out that the cycles analyzed herein cover always the first three months of each year, while year 2006 SLAs, already analyzed with JASON1 (cycles 147-149), are studies with ENVISAT as well (cycles 44-47). Note that the SLA varia- tions presented by JASON1 are not directly comparable with those of ENVISAT, since they refer to different time scales, the former presenting a variation between 10 and 30 days and the latter a variation between 35 and 105 days.

Figures 10 and 11 present the available SLAs for pass 399 and cycles 23, 24 and 25 as well as their differences. In all Figures the horizontal axis refers to geographic latitude and the vertical one to SLAs or SLA differences in m. From Figure 10 (top) a mean separation between the repeated ENVISAT cycles is evidenced, of the order of ~10 cm, while if this bias is neglected, the SLA records follow the same periodic pattern of decreased and increased sea level with increasing latitude. Therefore, it is expected that a trend within these three cycles would not be evident. This is confirmed from Figure 11, where the SLA differences between cycles 23, 24 and 25 are presented, since the estimated trends are between +4 mm/35-days and -2 mm/35-days.

From Figure 10 (bottom) where the respective SLAs for cycles 33, 34 and 35 are plotted, it is interesting to notice that cycle 34 misses a significant number of records compared to the other, so that no data are available north of $\varphi=39.5^o$. Moreover, cycle 34 follows closely the other two cycles analyzed until $\varphi=34.3^o$ (approximately at the south-east corner of Crete), and as the satellite moves to northern latitudes it deviates significantly with a bias of the order of ~15-20 cm. This is a good indication that the available SLA records from that cycle contains blunders, since when investigating the mean wind-speed for each cycle it was found that they do not deviate significantly (the wind speed ranges between 6.6 m/s, 10.7 m/s and 7.2 m/s for cycles 33, 34 and 35 respectively). Therefore, wind-drives SLA variations that were not treated by the applied IB correction cannot be blamed for the deviations found. When investigating the differences between the three cycles (see Figure 12) it is found that a positive trend of +6 mm/35-days exists between cycles 34 and 35, while a negative trend of –5 mm/35-days exists between cycles 33 and 34. As a consequence, no trend is found in the 3-month period covered by cycles 33 and 35.

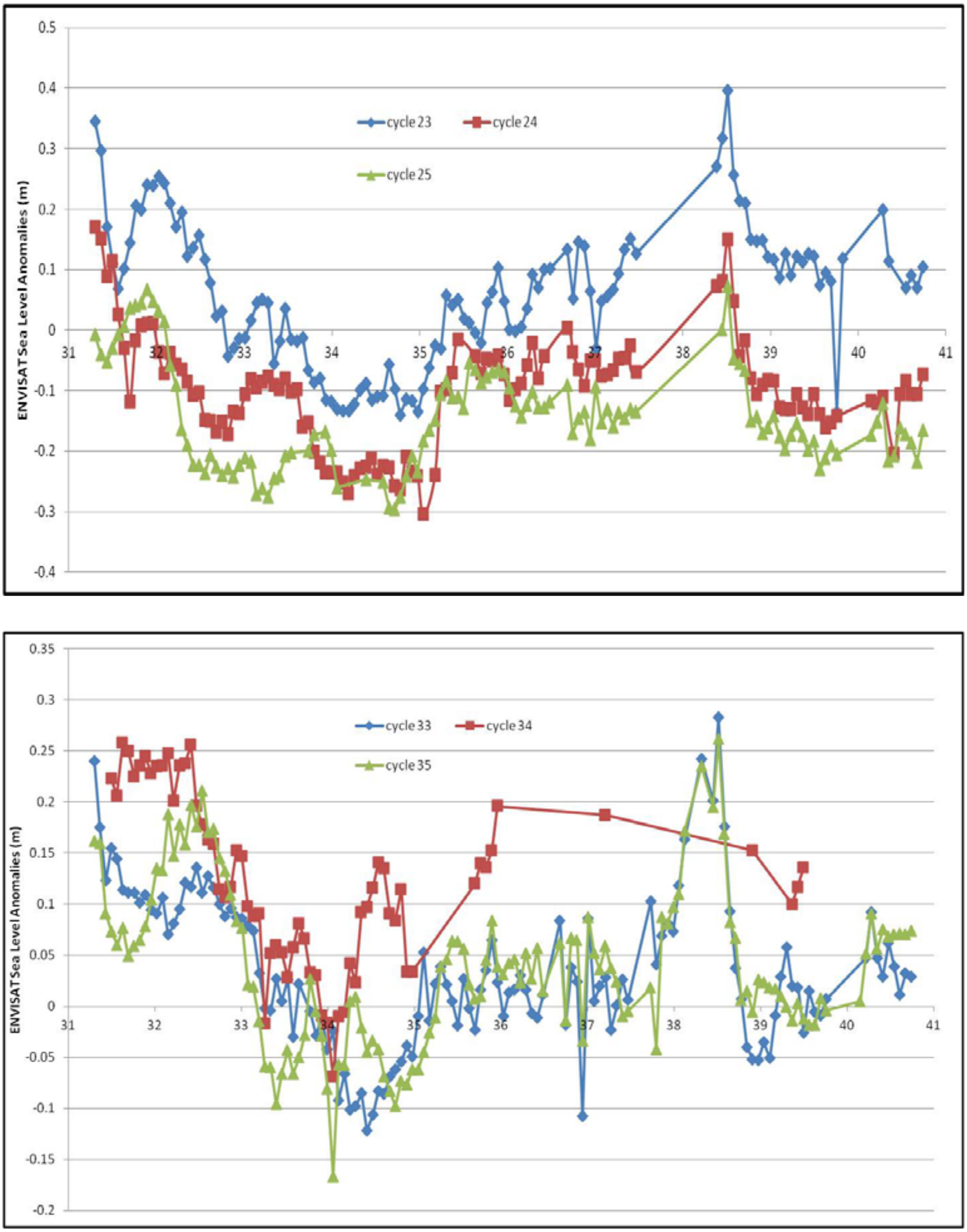

Figure 10. **ENVISAT pass 399 SLAs for cycles 23, 24 and 25 (top), cycles 33, 34 and 35 (bottom).**

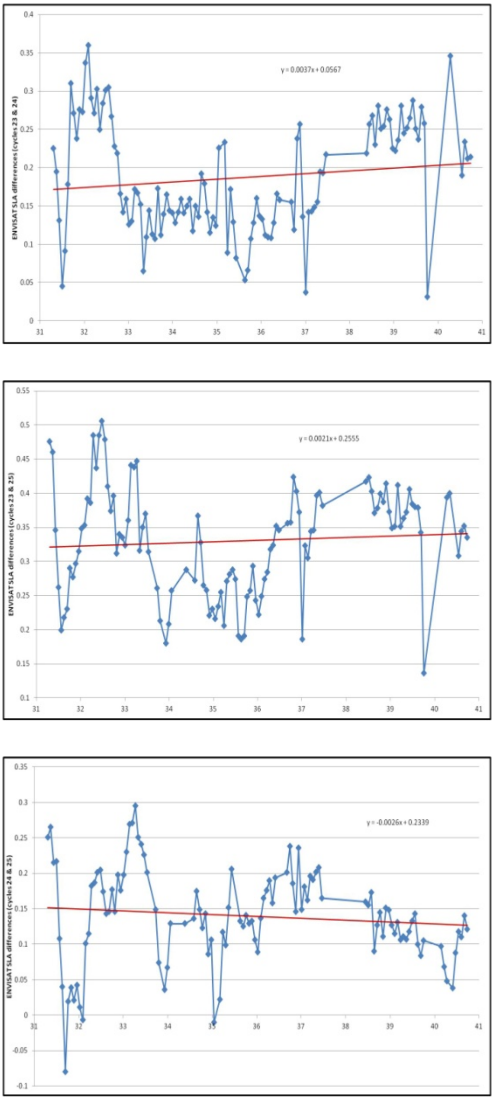

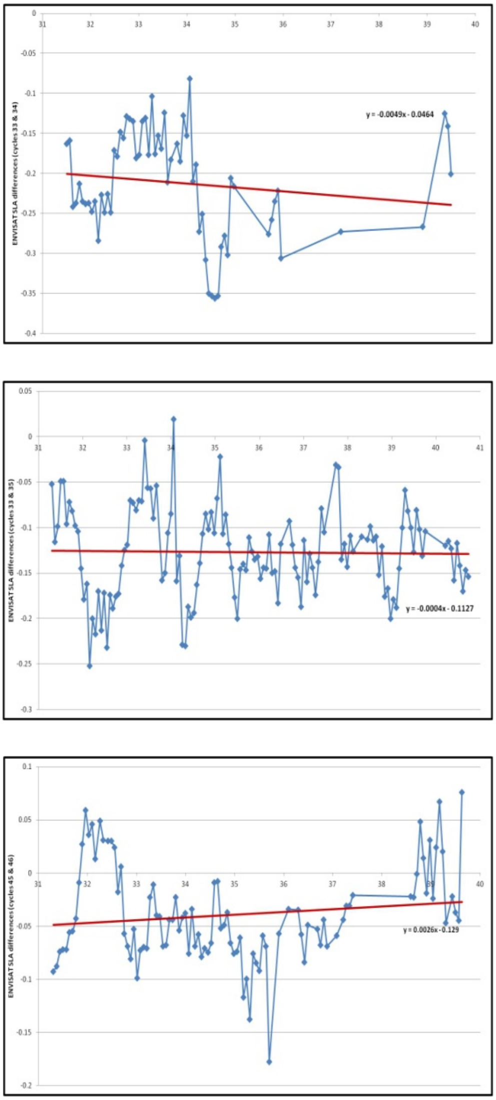

Figure 11. **ENVISAT SLA differences and linear trend for pass 399 between cycles 23 and 24 (top), 23 and 25 (middle), 24 and 25 (bottom).**

Figure 12. **ENVISAT SLA differences and linear trend for pass 399 between cycles 33 and 34 (top), 33 and 35 (middle), 34 and 35 (bottom).**

Figure 13 below, presents the SLA records for cycles 44, 45 and 46 covering the first three months of 2006, where an interesting agreement is found between the consecutive records of the satellite. This signals that almost no bias exists between the SLA records, since this is at the 5 cm level at most. Once again, one cycle misses a significant number of records, that is cycle 46, since no SLA data are available north of $\varphi=39.6^o$. Nevertheless, the same problems as with cycle 34 are not evidenced for the rest of the cycle records, since they do not present any extreme, blunder-like, variations compared to cycles 44 and 45. From that analysis of the differences between the SLAs (see Figure 14), a zero trend is found between cycles 44 and 45, while the sea rises by+2 mm/35-days between cycles 45 and 46, so that the same trend holds between cycles 44 and 46 as well.

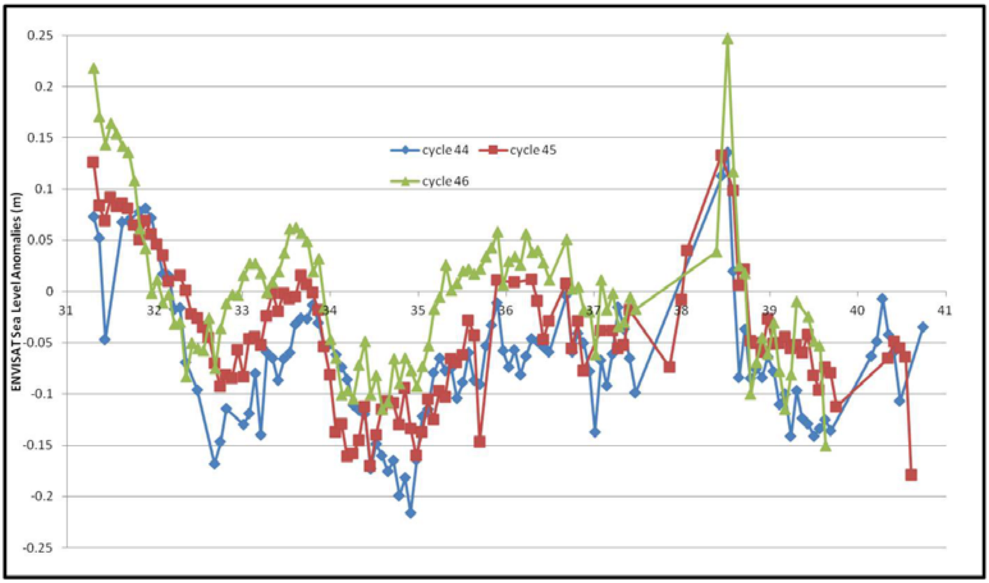

Figure 13. **ENVISAT pass 399 SLAs for cycles 44, 45 and 46.**

It is quite interesting to investigate the possible correlations between ENVISAT and JASON1 SLAs that belong to approximately the same time period and examine is the same level of SLA trend is derived. As it was presented in Figure 4, the ENVISAT and JASON1 tracks do not cover the same geographical area, while the ocean circulation pattern in the Adriatic Sea and the Aegean Sea are quite different. Nevertheless, it would be interesting to investigate if this collocated analysis can give some meaningful results.

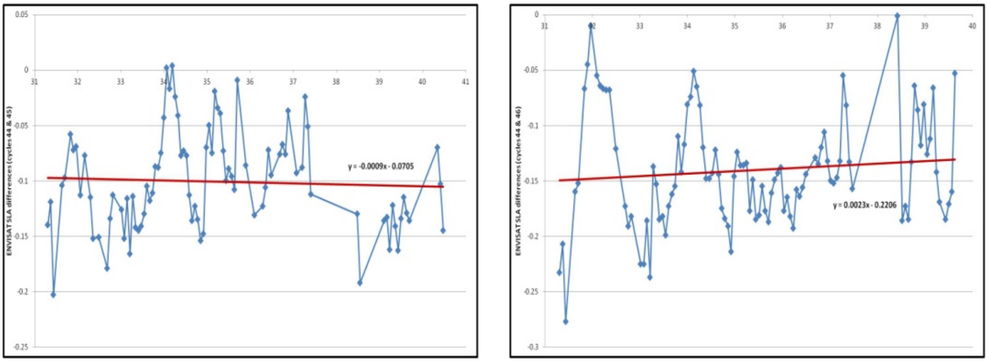

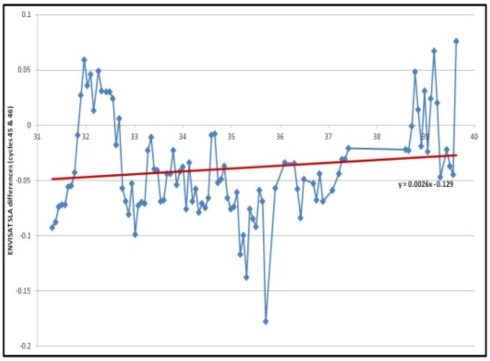

Figure 14. **ENVISAT SLA differences and linear trend for pass 399 between cycles 44 and 45 (top right), 44 and 46 (top left), 45 and 46 (bottom).**

Figure 15 presents the SLAs from the respective satellite records, where a very good agreement can be found between JASON1 and ENVISAT. It should be noted that the SLA records plotted in that Figure refer to the original location of each satellite, so no interpolation to a mean latitude has been performed in order to maintain the inherent accuracy of the data. This good agreement can be also viewed in the determined correlation coefficient between the SLA records, which is at the 50.2% level. If one considers that the available records refer to different locations, which are ~350 km apart, it becomes evident that the combined analysis of multi-mission altimetry data at collocated epochs can lead to an improved analysis of the variations of the sea level. In terms of the determined SLA trends, a very good agreement was once again found, since JASON1 records give a trend of +0.9 mm compared to 0.3 mm for ENVISAT. Given the error budget of satellite altimetry, it is evident that both satellites determine a zero level trend for the period investigated, confirming their good agreement.

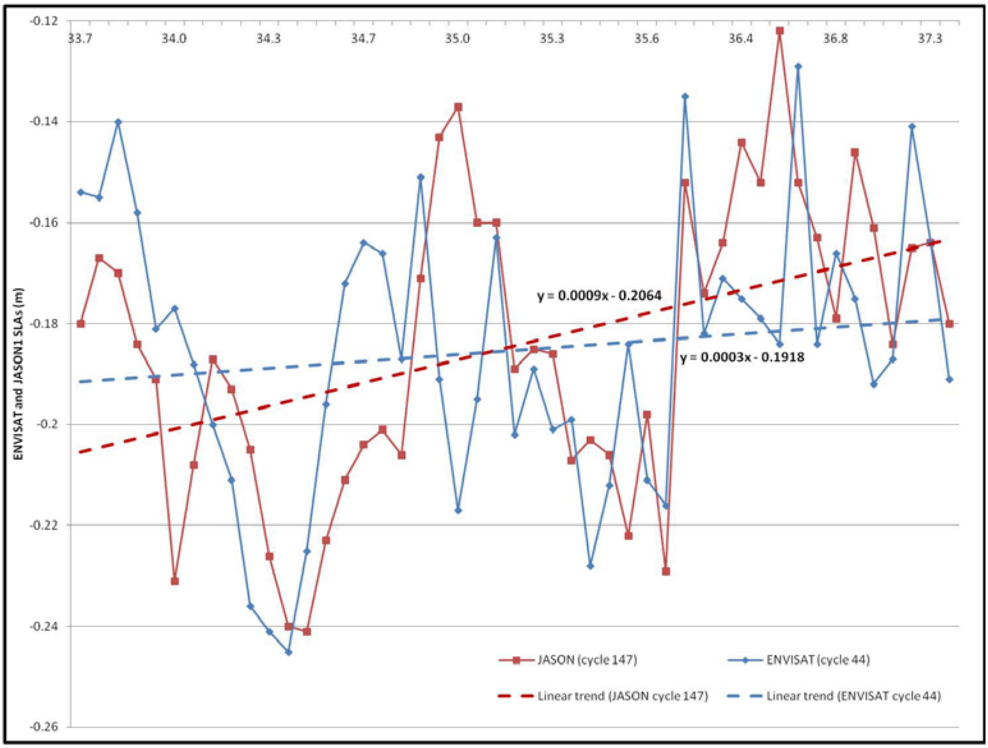

Figure 15. **SLAs from ENVISAT cycle 147 along pass 399 and JASON1 cycle 44 along pass 109.**

4. Mean sea surface model development

Following the analysis of the JASON1 and ENVISAT SLAs, the available data have been used to determine a Mean Sea Surface (MSS) model for the Mediterranean Sea. Given that the SLA records are referenced to the EGM2008 model (Pavlis et al., 2008) the contribution of that global geopotential model, full to degree and order 2159, has been evaluated to the final MSS grid nodes. The final model was selected to have a 5′×5′ spatial resolution, therefore EGM2008 geoid heights have been estimated to that grid in the zero-tide system in order to conform with the tide conventions adopted for the altimetric data processing. Table 6 presents the statistics of the EGM08 contribution to geoid heights for the area under study, which covers the entire Mediterranean Sea.

In order to determine the MSS model, the available SLAs from JASON1 and ENVISAT after the 3σ test have been used (see Table 3). These SLAs are utilized in the frame of LSC in order to estimate the 5′×5′ MSS model, so first the empirical covariance function has been estimated in order to derive the necessary parameters, which were then used to estimate the SLA on the required reference grid. Figure 16

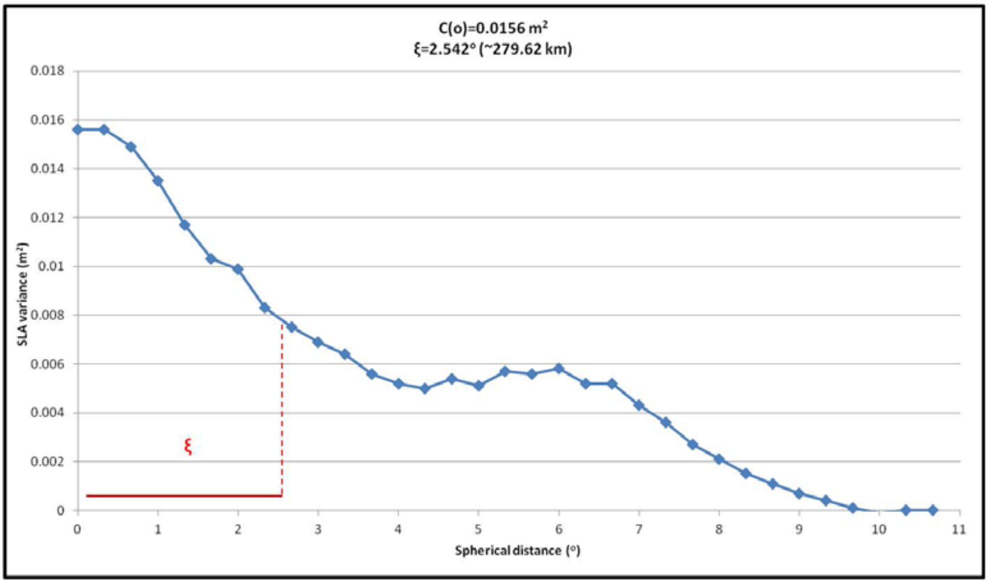

Figure 16. **Combined JASON1 and ENVISAT SLA empirical covariance function.**

below presents the empirical covariance function of the combined, multi-satellite SLA dataset, from which a variance of 0.0156 m^2 and a correlation length of ~280 km were found.

Table 6: Statistics of a) the EGM2008 contribution to geoid heights for the area under study, b) the final MSS model and c) its differences with DTU2010. Unit: [m].

	min	max	mean	std
EGM2008	-0.906	59.401	37.780	±12.413
MSS (5′×5′)	0.847	59.527	37.818	±12.374
MSS-DNSC08	-2.527	0.743	0.002	±0.080

The evaluation of the empirical covariance function and the subsequent fit of the Tscherning and Rapp model (Tscherning and Rapp, 1974) to these empirical values have been evaluated with the Gravsoft suite of programs (Forsberg and Tscherning, 2008). Using the parameters determined from the fit of the analytical model (i.e., depth to Bjerhamar sphere, fitted variance and scale factor), together with the error degree variances of the EGM2008 model, the final LSC-based prediction on the 5′×5′ nodes has been carried out. Finally, the MSS model has been determined by restoring the contribution of EGM2008. Table 6, middle row, summarizes the statistics of the estimation MSS model for the Mediterranean Sea, while the model itself is depicted in Figure 17.

In order to evaluate the estimated MSS model, a comparison with the latest Mean

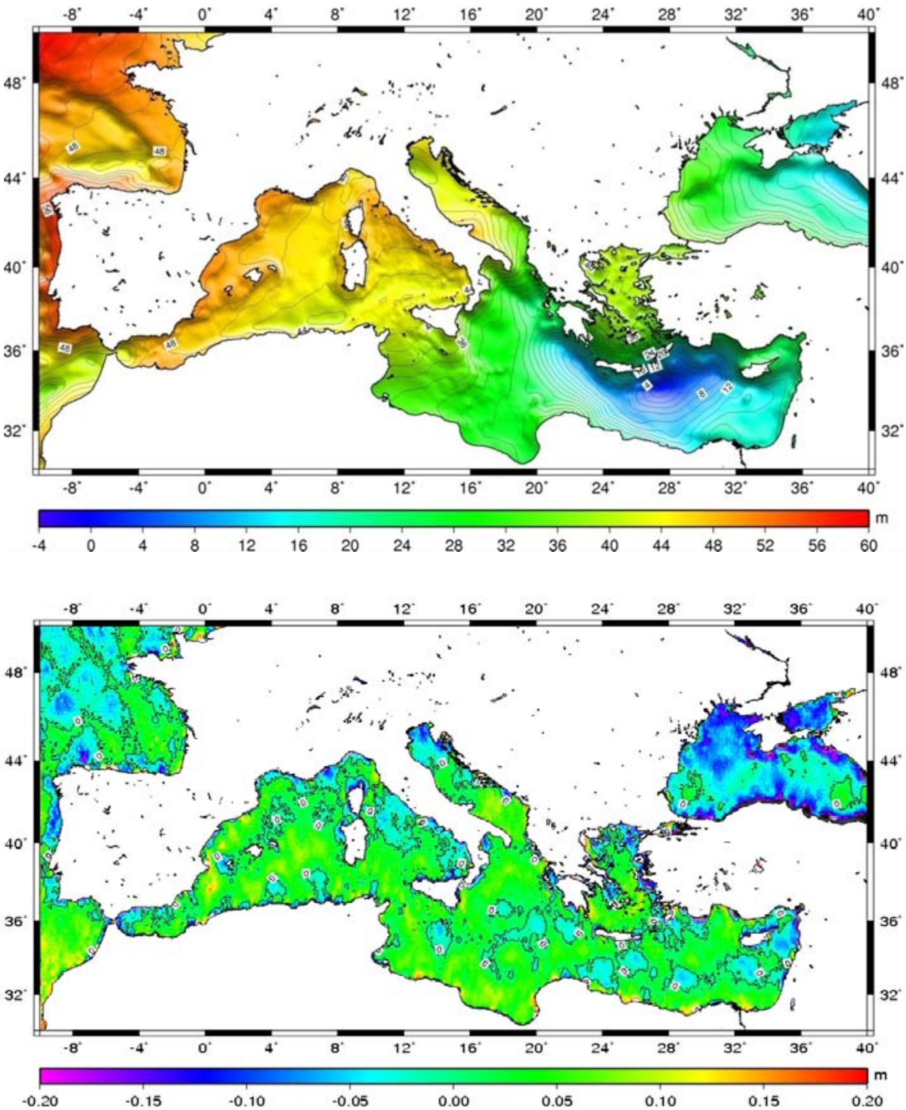

Figure 17. **The final combined JASON1 and ENVISAT MSS model from LSC (top) and its differences with DTU2010 (bottom).**

Sea Model from the Danish Space Agency, namely DNSC2010 (Andersen 2010, Anderse and Knudsen 2009) has been carried out. The statistics of the differences are presented in Table 6 (last row) which Figure 17 (bottom) depicts them for the entire area under study. As it can be seen from both the Table and the Figure, the statistics are quite satisfactory, since the std of the differences is at the ±8 cm level only, with the mean value almost at zero. In purely marine areas, the developed MSS model agrees vary well with DNSC2010 (all differences between -5 and 5 cm), while the largest deviations are found only along coastal areas, where special retracked altimetric data have been used in DNSC2010. Such data and processing methodologies have not been considered in the developed MSS model, therefore such large differences in coastal areas are expected. If a mask of 20 km is used around the coastline, in order to consider purely marine areas, then the std of the differences reduces to 4 cm only and the range is between -50 and 50 cm. This is good evidence that the so-derived MSS model is comparable with global ones, which are based on far more data sources (practically all available satellite altimetry data are used, from GEOSAT and ERS1 to JASON2 and ENVISAT) and sophisticated data treatment.

5. Conclusions

An analytical outline of the use of satellite altimetry data from the exact repeat missions of JASON1 and ENVISAT to monitor SLA variations has been presented. The study referred to the detection of trends in the sea level, either rise or fall, for short time periods between 10 and days and 3 months, based on geophysically and IB corrected altimetric records. The data analyzed referred to along-track records for two tracks that span the entire Mediterranean Sea in the north-south direction. From that analysis, trends between -2 cm/10-days and 3 cm/10-days have been determined, showing that the sea level has significant variations, which are not wind and/or pressure driven, even at such small time intervals.

When longer time intervals of the order of 35-days to 3-months are investigated, these trends are significantly reduced, something expected since short-time variations are smoothed out. In that case the trends determined from ENVISAT data are of the order of ~3-6 mm per 35-days to 3-motnhs and are in agreement with the 20-year long global trends identified from the analysis of all available altimetric records. The available along-track JASON1 and ENVISAT SLAs, have then been used to determine a Mediterranean-wide MSS model. The estimation was based on LSC for the prediction of the SLA on the final $5' \times 5'$ nodes, while the resulting model presents a very good agreement with the latest global MSS model, namely DTU2010. The standard deviation of the developed MSS with DTU2010 is at the ±8 cm level, while when purely marine areas are considered, after the application of a 20 km wide coastline mask, it reduced to ±4 cm only.

References

Andersen O B (2010) The DTU10 Gravity field and Mean sea surface (2010). Second international symposium of the gravity field of the Earth (IGFS2010), Fairbanks, Alaska.

Andersen OB, Knudsen P (1998) Global marine gravity field from the ERS1 and Geosat geodetic mission. J Geophys Res 103: 8129-8137.

Andersen OB and Knudsen P (2009) The DNSC08 mean sea surface and mean dynamic topography. J Geophys Res 114(C11) doi:10.1029/2008JC005179.

Arabelos D, Tziavos IN (1996) Combination of ERS1 and TOPEX altimetry for precise geoid and gravity recovery in the Mediterranean Sea. Geophys J Int 125: 285-302.

AVISO User Handbook (1998) Corrected Sea Surface Heights (CORSSHs) AVI-NT-011-311-CN Edition 31.

AVISO (2011) Available from: http://www.aviso.oceanobs.com/en/altimetry/principle/basic-principle/. Accessed October 2011.

Barzaghi R, Maggi A, Tselfes N, Tsoulis D, Tziavos IN, Vergos GS (2009a) Combination of Gravimetry, Altimetry and GOCE Data for Geoid Determination in the Mediterranean: Evaluation and Simulation. In: Sideris MG (ed) Observing our Changing Earth, International Association of Geodesy Symposia Vol. 133, Springer Berlin Heidelberg New York, pp. 195-202.

Barzaghi R, Tselfes N, Tziavos IN, Vergos GS (2009b) Geoid and High Resolution Sea Surface Topography Modelling in the Mediterranean from Gravimetry, Altimetry and GOCE Data: Evaluation by Simulation. Journal of Geodesy, 83(8):751-772. doi: 10.1007/s00190-008-0292-z.

Cazenave A and Nerem RS (2004) Present-day sea-level change: Observations and causes. Reviews in Geophysics 42 (RG3001), doi:10.1029/2003RG000139.

Cazenave A, Schaeffer P, Berge M, Brosier C, Dominh K, Genero MC (1996) High-resolution mean sea surface computed with altimeter data of ERS1 (geodetic mission) and TOPEX/POSEION. Geophys J Int 125: 696-704.

Chelton DB, Ries JC, Haines BJ, Fu LL, Callahan P (2001) Satellite Altimetry. In: Fu LL, Cazenave A (eds) Satellite Altimetry and Earth Sciences A Handbook of Techniques and Applications. International Geophysics Series 69: 1-132, Academic Press, San Diego, California.

Church JA, White NJ, Konikow LF, Domingues CM, Cogley JG, Rignot E, Gregory JM, van den Broeke MR, Monaghan AJ, Velicogna I (2011). Revisiting the Earth's sea-level and energy budgets from 1961 to 2008. Geophys Res Lett (38) L18601. doi:10.1029/2011GL048794.

Fernandes JM, Barbosa S, Lázaro C (2006) Impact of Altimeter Data Processing on Sea Level Studies. Sensors (6): 131-163.

Forsberg R and Tscherning CC (2008) An overview manual for the GRAVSOFT Geodetic Gravity Field Modelling Programs. 2nd ed.

Naeije M, Scharroo R, Doornbos E, Schrama E (2008) GLobal Altimetry Sea-level Service: GLASS. Final Report. NIVR/DEOS publ., NUSP-2 report GO 52320 DEO, 107pp, December 2008.

Natsiopoulos DA (2010) Determination of mean sea surface and sea level anomaly models in different regional and temporal scales by altimetric data. Diploma Theses, Department of Geodesy and Surveying, Aristotle University of Thessaloniki, Greece, June 2010.

Nerem RS, Leuliette E, Cazenave A (2006) *Present-day sea-level change: A review.*

Comptes Rendus Geosciences, 338, 1077-1083.

Nerem RS, Mitchum GT (2001) Sea Level Change. In: Fu L.-L. and Cazenave A (eds) Satellite Altimetry and Earth Sciences. Int Geophys Series Vol 69, Academic Press, San Diego California, 329-350.

Pavlis NK, Holmes SA, Kenyon SC, Factor JK (2008) An Earth Gravitational Model to Degree 2160: EGM2008, presented at the 2008 General Assembly of the European Geosciences Union, Vienna, Austria, April 13-18, 2008.

RADS-DEOS (2011) Available from: http://rads.tudelft.nl (Radar Altimeter Database System). Accessed January 2011.

Sansò F, Venuti G, Tziavos IN, Vergos GS, Grigoriadis VN (2008) Geoid and Sea Surface Topography from satellite and ground data in the Mediterranean region - A review and new proposals. Bulletin of Geodesy and Geomatics 67(3): 155-201.

Tapley BD, Kim M.-G. (2001) Applications to Geodesy. In: Fu L.-L. and Cazenave A (eds) Satellite Altimetry and Earth Sciences. Int Geophys Series Vol 69, Academic Press, San Diego California, 371-406.

Tscherning CC, Rapp (1974) Closed Covariance Expressions for Gravity Anomalies, Geoid Undulations, and Deflections of the Vertical Implied by Anomaly Degree-Variance Models. Rep of the Dept of Geodetic Sci and Surv No 208 The Ohio State Univ, Columbus, Ohio.

Tziavos IN, Forsberg R, Sideris MG (1998) Marine Gravity Field modelling Using Shipborne and Geodetic Missions Altimetry Data. Geomatics Research Australasia, No.69:1-18.

Tziavos IN, Vergos GS, Kotzev V, Pashova L (2005) Mean sea level and sea surface topography studies in the Black Sea and the Aegean. International Association of Geodesy Symposia, Vol. 129, Jekeli C, Bastos L, Fernandes J (eds.), Gravity Geoid and Space Missions 2004, Springer – Verlag Berlin Heidelberg: 254-259.

Vergos GS (2002) Sea Surface Topography, Bathymetry and Marine Gravity Field Modelling. UCGE Rep Nr 20157, Calgary AB, Canada.

Vergos GS, Tziavos IN, Andritsanos VD (2005a) On the Determination of Marine Geoid Models by Least-Squares Collocation and Spectral Methods Using Heterogeneous Data. In: Sansó F (ed.) A Window on the Future of Geodesy, Inter Assoc of Geod Symposia, vol. 128, Springer – Verlag Berlin Heidelberg, 332-337.

Vergos GS, Tziavos IN, Andritsanos VD (2005b) Gravity Data Base Generation and Geoid Model Estimation Using Heterogeneous Data. In: Jekeli C, Bastos L, Fernandes J (eds.) Gravity Geoid and Space Missions 2004, Inter Assoc of Geod Symposia, vol. 129, Springer – Verlag Berlin Heidelberg, 155-160.

Vergos GS, Grigoriadis V, Tziavos IN, Sideris MG (2007) Combination of multi-satellite altimetry data with CHAMP and GRACE EGMs for geoid and sea surface topography determination. In: Tregoning P, Rizos C (eds) Dynamic Planet 2005 - Monitoring and Understanding a Dynamic Planet with Geodetic and Oceanographic Tools, International Association of Geodesy Symposia, vol.130 Springer – Verlag Berlin Heidelberg, pp. 244-250.

Yi Y (1995) Determination of gridded mean sea surface from altimeter data of TOPEX, ERS-1 and GEOSAT. Rep of the Dept of Geodetic Sci and Surv No 434 The Ohio State Univ, Columbus, Ohio.